

Public justification (visible to the public if the article is accepted and published):

The reviewer comments and criticisms have been adequately answered in the revised manuscript, however some specific points concerning fluid dynamical details etc. should be further refined in the final manuscript.

Additional private note (visible to authors and reviewers only):

Dear Authors,

while I think the reviewer comments and criticisms have been adequately answered in the revised manuscript I need to ask you to clarify some additional points that are not clearly explained in my view.

We thank the editor for diligently reviewing the manuscript and providing detailed comments. We hope to adequately address the remaining concerns with the point-by-point replies below and **modifications to the manuscript.**

1. Line 127 states that the model assumes laminar flow but for my understanding this is not given at the involved flows and geometries. The entrance length for either IMR is in excess of 1m, so a laminar profile will not at all be developed at the end of the concentric flow part of the Eisele-IMR nor at the orifice of both IMRs. The effect of the flow profiles for the resulting profile shown in Fig.8 and the final results should be discussed.

We agree that the entrance length for both IMRs exceeds 1 m (under the assumption of laminar flow) and agree with the conclusion that there is often not enough time in the different inlet sections for the laminar flow to completely develop into a fully developed laminar flow profile, including the volumes close to the orifices. As we understand the comment, the editor's principal concern seems to be whether the flow profiles at the merging of the sheath and sample flow (new Fig. 8) are reasonable. The velocity profile of the sample flow entering the sample tube is model-initialised as fully developed. This is justified if an appropriate sampling tube extending the inlet is used in actual measurements. We amend the description of the model setup accordingly.

The initial flow profile of the sheath flow (at the very left of the geometry shown in Fig. 7) is likewise model-initialised as fully developed. In reality, the profile - resulting from the provision of the sheath gas through tubing, a hole-filled plate ("shower head"), and finally a laminarising mesh - is somewhere between a plug and parabolic flow profile. While the assumption of a fully developed flow is arguably less accurate for this very initial section of the sheath flow, we deem that this does not limit the overall accuracy of the modelling further downstream. Figure 8 shows how the initially parabolical sheath flow profile (for the entire radial range 9–22 mm) splits into two fairly parabolic profiles (9–15 mm and 16–22 mm, divided by the "ion cage electrode") over the distance of several cm only. The reason for the relatively fast development of the profiles is the close distance (5 mm) between the surfaces, equivalent to an entrance length of many cm only. The model does not assume a fully developed laminar flow in this section (or elsewhere), the resulting flow profiles are merely the result of the modelled shear forces under the assumption of laminar flow. We conclude that assuming an initially fully developed laminar sheath flow does not present a limitation, and do not think there is a fundamental issue with the study.

Multiple adjustments that aim for more clarity in the text include:

Section 3.1, MION2 inlet, line 166 in change-tracked manuscript:

Assuming an interface upstream of the MION2 inlet that creates a fully developed laminar flow, ...

Section 3.2 Eisele type inlet, line 224 in change-tracked manuscript:

The initial sample flow velocity profile is assumed to be fully developed, assuming an appropriate interface upstream of the inlet. The sheath flow profile, initialised likewise as fully developed laminar flow, quickly adjusts to the concentric tubing geometry.

2. Since it is far from easy to quantitatively generate dilute H₂SO₄ mixtures the procedure used should be at least given and referenced. The consequences for the reported sensitivities should be discussed as well.

We would like to clarify that H₂SO₄ was not used in any experiments within this study, only in the modelling. In the modelling, H₂SO₄ is used as a prototypical molecule that clusters with the reagent ion. The abundance of the H₂SO₄ in the sample gas does not matter and will only proportionally affect the abundance of the formed cluster, as long as there is no substantial reagent ion depletion. We intend to make this clearer with a few minor changes in the manuscript.

(1) Section 2.2 now elaborates on why the dilute concentration was chosen.

As proxy for target molecules, dilute sulfuric acid H₂SO₄ is modelled to be contained in the sample flow at a mixing ratio of 1 ppt. It reacts kinetically with Br⁻ and NO₃⁻ to form H₂SO₄.Br⁻ and H₂SO₄.NO₃⁻. The magnitude of the H₂SO₄ abundance is not critical for the interpretation of the modelling results, as long as the clustering with the reagent ion does not substantially reduce the reagent ion concentration.

(2) Section 2.3 Laboratory measurements:

H₂SO₄ or other targets gases were not employed in the laboratory experiments but treated in the modelling only.

(3) We have amended the captions of Fig. 1 and Fig. 7 to now indicate that the figures show modelled physical quantities, not measured physical quantities.

Minor issues:

1. For the MION2 length should be also given at the beginning of section 3.1, now it is only introduced somewhere later in the text. The basic geometry data of both IMRs could also be included in Table 1 for convenience. Fig. 1 itself does not give any details (line 160).

We now specify the length of the MION2 and Eisele IMR, in addition to the IMR diameter, in the respective sections 3.1 and 3.2. We are happy to follow the suggestion to add the information in Table 1.

2. I would find it interesting to see the downstream circular cross sections of the product ions few cm in front of the orifices within Figs. 1 and 7.

The model framework allows to extract this information. The reagent ions distribution is the following.

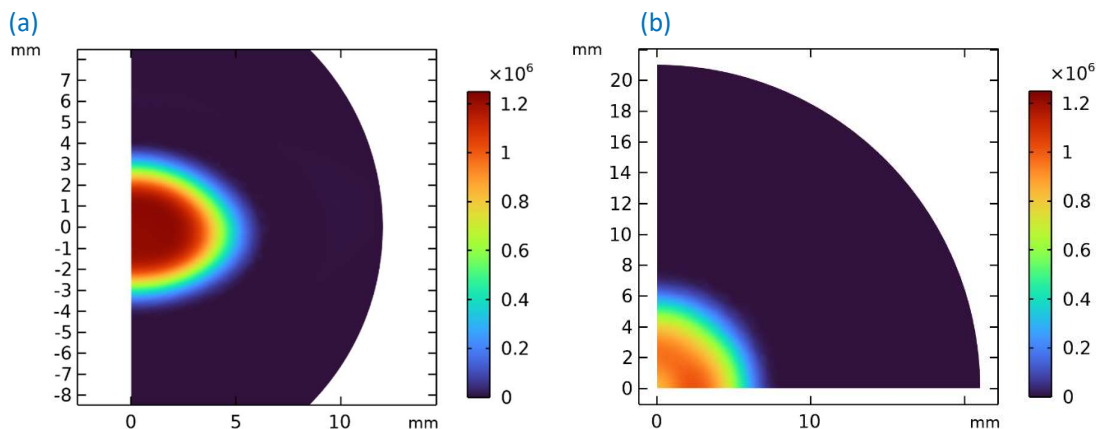


Figure R1: Reagent ion concentrations (NO_3^- , $[\text{cm}^{-3}]$) 5 mm in front of the orifice plate, for MION2 (a) and Eisele-type inlets (b). The axes indicate the radial distance [mm]. The distribution is essentially rotationally symmetric for both inlets. In MION2, the ion beam is marginally compressed in the y-direction (the direction of ion injection into the IMR).

The distribution of cluster ions is of similar to that of the reagent ions, given that the reaction time between the target gas and the reagent ion is approximately path independent up close to the orifice. We deem the information that Fig. R1 could add to the manuscript too little to warrant the inclusion of such a dedicated figure in the manuscript. Likewise, we are reluctant to add the cross sections as additional panels to figures 1 and 7, as it would make the figures even more busy than what they already are. However, based on the editor suggestion, we consider it prudent to include the cross sections in Fig. 4 – in which the change of the cross-section area of the ion plume is discussed – and briefly discuss the rotational symmetry in the main text. The base value of U_A in Fig. 4 was updated to -1500 V (previously -3000 V), to be directly comparable to Fig. 1.

Line 199 of the change-tracked manuscript:

If chosen correctly, the electro-advective streamlines connect the pinhole and the ionisation volume (Figure 1d), and the distribution of ions in the IMR close up to the pinhole is essentially rotationally symmetric. The marginal beam compression in the ion injection direction is due to the advective velocity being largest in the plane of injection.

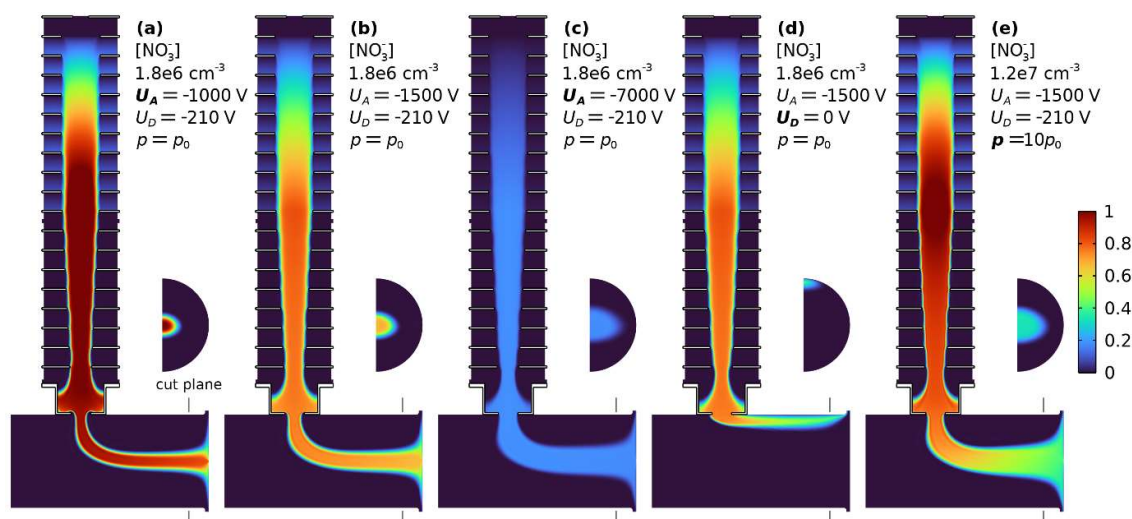


Figure 4: Sensitivities of NO_3^- concentrations in MION2 inlet to different acceleration voltages U_A (a-c), deflector voltage $U_D=0$ V for deactivation (d), and primary ion production rate (e). The semi circle areas show the ion concentration in the cut plane 5 mm in front of the orifice. The colour scale ranges from 0 to the maximum described in each panel. Figures a-d use the same colour scale. The width of the ion beam increases for larger voltages, while the extracted concentrations slightly decrease. At concentrations of 10^7 cm^{-3} space charge leads to a spreading of the ion beam, the concentration at the pinhole is lower than at the ionisation volume.